

0202
SPB-74
5.1.1
6.1.1

APPLICATION OF PHASE SHIFTED, LASER FEEDBACK INTERFEROMETRY TO FLUID PHYSICS

6.1.1

Ben Ovryn¹, Steven J. Eppell², James H. Andrews³ and John Khaydarov⁴

¹NYMA Inc. NASA Lewis Group
NASA Lewis Research Center, MS 110-3
21000 Brookpark Road
Cleveland, Ohio 44135
ovryn@wave.lerc.nasa.gov

²Department of Biomedical Engineering
Case Western Reserve University
Cleveland, Ohio 44106
^{3,4}Ohio Aerospace Institute
³Currently with: Department of Physics
Youngstown State University

ABSTRACT

We have combined the principles of phase-shifting interferometry (PSI) and laser-feedback interferometry (LFI) to produce a new instrument that can measure both optical path length (OPL) changes and discern sample reflectivity variations. In LFI, coherent feedback of the incident light either reflected directly from a surface or reflected after transmission through a region of interest will modulate the output intensity of the laser. LFI can yield a high signal-to-noise ratio even for low reflectivity samples.

By combining PSI and LFI, we have produced a robust instrument, based upon a HeNe laser, with high dynamic range that can be used to measure either static (dc) or oscillatory changes along the optical path. As with other forms of interferometry, large changes in OPL require phase unwrapping. Conversely, small phase changes are limited by the fraction of a fringe that can be measured. We introduce the phase shifts with an electro-optic modulator (EOM) and use either the Carre or Hariharan algorithms to determine the phase and visibility.

We have determined the accuracy and precision of our technique by measuring both the bending of a cantilevered piezoelectric bimorph and linear ramps to the EOM. Using PSI, sub-nanometer displacements can be measured. We have combined our interferometer with a commercial microscope and scanning piezoelectric stage and have measured the variation in OPL and visibility for drops of PDMS (silicone oil) on coated single crystal silicon. Our measurement of the static contact angle agrees with the value of 68° stated in the literature.

INTRODUCTION

Optical response of the laser feedback interferometer

The optical response of the laser with external feedback is in general a nonlinear function of the reflectivity of the object and the variation in the optical path length. The governing model (Figure 1) considers the reflection from the sample (M_3) as forming a Fabry-Perot interferometer with the output mirror of the laser (M_2). Our model for the modulation of the irradiance of the cavity neglects the finite response time of the laser cavity (an assumption which is valid in our experiments), assumes that the reflectivity, R_2 , of the laser mirror (M_2) is close to unity and includes the possibility of multiple reflections from the sample. The irradiance in the interferometer, which is a function of the reflectivity of the sample and the optical path length, $\delta(t)$, is given as (for details of the derivation see Ovryn et. al.)¹:

$$I(m, \delta(t)) = I_0 \left(1 + m \sum_{i=1}^{\infty} (R_2 R_3)^{\frac{i-1}{2}} \cos \left(\frac{i4\pi}{\lambda} \delta(t) + \Psi \right) \right) \quad (1)$$

where $\delta(t)$ is the change in the optical path length (OPL), Ψ represents an arbitrary overall phase factor, I_0 is the average laser irradiance, and m is the modulation parameter (fringe visibility) which is given as:

$$m = \gamma \sqrt{R_3} \quad (2)$$

where γ is a function of the reflectivities of the laser mirrors and intrinsic laser parameters. Significantly, it can be

observed that the fringe modulation is directly proportional to the amplitude reflectivity of the object. When multiple reflections from the object can be ignored only the first term in the summation is significant and the response of the interferometer, Eq. 1, simplifies to:

$$I(m, \delta(t)) = I_o (1 + m \cos (\frac{4\pi}{\lambda} \delta(t) + \Psi)) \quad (3)$$

For a d.c. and oscillatory change in OPL, $\delta(t) = n(a + b \sin \omega t)$, Eq. 1 yields, ($\Psi = 0$):

$$I(\omega, t) = I_o (1 + m (\cos (2kna) J_0 (2knb)) - 2 \sin (2kna) J_1 (2knb) \sin (\omega t) + 2 \cos (2kna) J_2 (2knb) \sin (2\omega t) - \dots) \quad (4)$$

Phase shifting interferometry

When multiple reflections are negligible, the interferometer response of Eq. 3 is the standard form for a two beam interferometer. In this case, phase shift methods can be applied to determine the OPL and the fringe visibility. In phase shifting interferometry (PSI) a series of experimentally controlled optical path length changes are introduced in order to solve for the sample's phase, $\phi(t)$, and visibility, $m(t)$ from a least squares solution to an over determined set of measurements.^{1,2} There are several algorithms which can be employed; in our work, we have used either the Carre or the Hariharan algorithm to solve for the phase and the visibility.^{1,2} The strength of using an over determined set of measurements is that a solution for the phase, $\phi(t)$, can be found which is independent of the other unknowns (I_o and m); similarly, a solution can be found for $m(t)$ which is independent of $\phi(t)$ and I_o . Since the phase is determined modulo 2π , the phase must be unwrapped in order to determine large changes in the OPL. Additionally, there is no ambiguity in the sign of the change in the OPL. As an illustration of this approach, consider the case where four phase shifts are used: $\Psi_1=0, \Psi_2=\pi/2, \Psi_3=\pi, \Psi_4=3\pi/2$. Substituting these phase steps into Eq. 3, produces a set of four equations:

$$\begin{aligned} I_1(t) &= I_o (1 + m(t) \cos \phi(t)) & I_3(t) &= I_o (1 + m(t) \cos (\phi(t) + \pi)) \\ I_2(t) &= I_o (1 + m(t) \cos (\phi(t) + \frac{\pi}{2})) & I_4(t) &= I_o (1 + m(t) \cos (\phi(t) + \frac{3\pi}{2})) \end{aligned}$$

Therefore:

$$\tan \phi(t) = \frac{I_2(t) - I_4(t)}{I_3(t) - I_1(t)} \quad I_o = \frac{(I_1(t) + I_2(t) + I_3(t) + I_4(t))}{4}$$

$$m(t) = \frac{\sqrt{(I_2(t) - I_4(t))^2 + (I_3(t) - I_1(t))^2}}{2I_o}$$

METHODS

There are several configurations that can be used to observe laser feedback effects. The laser power can be monitored by dividing the beam (using a beam splitter) from the front mirror of the laser or, as in our experiments, by monitoring the power of the beam which leaves the back mirror. In this simple configuration, the interferometer can be used for fringe counting. To achieve higher accuracy, we use an electro-optic modulator situated in the beam path between the front mirror of the laser and the object and employ PSI techniques.

Measurement of the harmonic response of the laser feedback interferometer

To verify the harmonic response of LFI, Eq. 4, we performed the following experiments. The light from a HeNe laser (Uniphase, 1107P), was modulated with an electro-optic modulator (New Focus, 4002 and New Focus, high voltage amplifier 3211) before passing through a pair of linear polarizers and illuminating a mirror mounted on a piezoelectric translator (Burleigh, PZ 81 with RC-44 driver). After reaching the mirror, the light was retro-reflected and re-entered the laser cavity. The power of the beam from the rear mirror of the laser was measured using a photodetector (New Focus, 1201 or 1801). The frequency and amplitude of the sinusoidal voltage to both the mirror and EOM were controlled independently by using a function generator (Stanford Research Systems, DS 340) and the source out on a spectrum analyzer (Stanford Research Systems, 770), respectively. The signal from the photodetector was sent directly to the spectrum analyzer and saved as a digitized waveform. In this configuration, changes in the optical path length could be achieved by changing the d.c. offset on the high voltage EOM amplifier.

Calibration of the phase shifting method using a piezoelectric bimorph

In order to prove the utility of the phase shift method as applied to LFI, we measured the cantilever bending of a piezoelectric bimorph; the bending of the bimorph is directly proportional to the applied voltage and is a quadratic function of the cantilever length.¹ Figure 2 presents a schematic of the apparatus used for this measurement. The bimorph was mounted in a clamp so that it formed a cantilever 20 mm in length. The clamp was attached to a uniaxial translation stage (UT 100, Klinger Inc.) which operated under closed loop control. A long working distance 50 x 0.42 NA objective (G Plan NIR, Mitutoyo, Inc.) was used to focus the laser spot on the surface of the bimorph.²

The phase was measured using the Carre algorithm with the four phase shifts introduced by applying discrete voltages to the electro-optic modulator. The phase shifts were controlled by a board inside a PC (DAS 1800HR, Keithley Inc.) which also acquired the voltage either directly from the photodetector; samples were digitized at 16 bits at up to 100 kHz. After acquiring the four phase shifts, the PC determined the phase, the visibility and I_0 on line. Our program also allows the user to average repeated phase measurements and provides the option of collecting many samples of the signal voltage from the photodetector at each phase shift and averaging. To determine the bending, the difference in phase before and after applying a voltage to the bimorph was obtained at various positions on the surface. The entire apparatus was mounted on a vibration isolation table and enclosed in a double Plexiglass box which reduced thermal drift and acoustical excitation; before data collection, the laser was at thermal equilibrium.

Measurement of random and systematic errors associated with the PSI-LFI method

To determine the random and systematic errors associated with the phase shift method, the bimorph was replaced with a small piece of single crystal silicon which was held fixed at the focus of the microscope objective. The change in phase due to a slowly varying (0.1 Hz) triangular wave applied to the EOM was measured for varying amounts of incident power on the sample; the magnitude of the ramp was set to provide a change in the optical path length of approximately 316 nm. To vary the power in the object beam, two polarizers were placed between the EOM and the back aperture of the microscope objective. A fixed linear polarizer was situated directly behind the EOM with orientation parallel to the polarization of the laser and a linear polarizer on a rotation stage (New Focus, 5524 and 8401) was placed between the first polarizer and the objective lens. The phase and visibility were measured using the Hariharan algorithm at several fixed settings of the rotatable polarizer as the power on the sample varied.

Measurement of the static contact angle of PDMS on coated silicon wafer

To produce high spatial resolution measurements over a whole field, we have combined our phase-shifted LFI with a piezoelectric stage which translated the sample along two axes under closed-loop control (S221, Queensgate, Inc.) and incorporated the instrument into a commercial microscope (Jenavert, Carl Zeiss).² We produced images of small drops of 60,000 cS PDMS (silicone oil) which were placed on a fluorinated (FC-723, 3M, Inc.) coated single crystal silicon wafer; the surface of the wafer was wiped with toluene and dipped into the barrier coat. Images were obtained by measuring the phase and visibility at discrete points on the drop and substrate with a 50 x 0.8 NA objective.

RESULTS

Harmonic response of the laser feedback interferometer

Figure 3 (left) shows the maximized first and second harmonics (top and bottom, respectively) when the EOM was modulated with a sinusoidal voltage at 2 kHz while the piezoelectric mirror remained stationary. The amplitude of the harmonic terms were controlled by varying the d.c. voltage (a in Eq. 4) to the EOM. These results illustrate that the even and odd harmonics are in phase quadrature.

Figure 3 (right) shows the LFI response when the EOM was modulated at 30 kHz and the mirror was oscillated at 3 kHz. Figure 3 (top, right) shows the effect of maximizing the LFI response at the fundamental frequency. In this case, both the 30 kHz EOM signal and the weaker 3 kHz signal from the mirror can be observed. An interesting effect is observed when the second harmonic response is maximized (Fig. 3, bottom, right); not only is the second harmonic of the EOM maximized at 60 kHz, but a response is observed at 33 and 27 kHz; this beating between the two frequencies can also be viewed as sum and difference frequency LFI, respectively.

Calibration of the phase shifting method using a piezoelectric bimorph

Figure 4 illustrates the measured bending of the piezoelectric bimorph for two separate voltages, 4.0 volts (insert) and -0.5 V. The data were acquired using four discrete phase shifts (with the Carre algorithm) and by obtaining the change in the optical path length cause by the applied voltage. Superimposed on each curve is a quadratic fit, which represents the predicted shape. The method unambiguously predicts the direction of the bending.¹

Measurement of random and systematic errors associated with the phase shift method

Figure 5 shows the variation in OPL and visibility due to phase drift during a 90 second period; the visibility was essentially constant during this time period. Systematic drift has also been observed.^{1,2} Figures 6 and 7 show the change in the optical path length (top) and fringe modulation (middle) due to a ramp applied to the EOM. In Figure 6, the average modulation was 0.0488; while in Figure 7, the maximum amount of light was allowed to pass through to the object. Also shown in Figures 6 and 7 is the difference in OPL between a half-period of the ramp and a least squares fit to the ramp (bottom curves). Periodic variations in the OPL (Fig. 7 bottom) and in visibility (Fig. 7, middle) can be observed for the higher visibility case. For the lower visibility case, the systematic errors no longer dominate and the rms phase error was 0.3 nm. The rms error in OPL calculated for a range of fringe visibilities indicates that the minimum error in the OPL (0.3 nm) was achieved for a visibility of 0.05.¹

Measurement of the static contact angle of PDMS on coated silicon wafer

Figure 8 show the variation in the optical path length (left) and the visibility (right), respectively, for a 26 μm diameter drop of silicone oil ($n= 1.447$). It can be observed that the visibility falls off very rapidly at the periphery of the drop. The static contact angle for this drop was calculated from twice the inverse tangent of the ratio of the height to the radius of the drop. The apex of the drop was determined to be 8.8 μm above the substrate and the diameter of drop was determined to be 26 μm . The contact angle of 68 $^\circ$ agrees with the literature.³

The measurement of the OPL requires not only a measurement of the phase, but also knowledge of the index of refraction of the fluid and a determination of the correction factor for the microscope objective. The correction factor for the objective was determined from the literature to be 1.26.⁴ We have not yet measured the accuracy of the correction factor for our microscope objective. Additionally, we have not yet determined the accuracy of the scanning stage; the closed loop stage has a stated precision of 5 nm.

DISCUSSION and CONCLUSIONS

We have designed a laser feedback interferometer which can be used to measure oscillatory and d.c. changes in the OPL. We have successfully combined the principles of PSI with LFI. We have measured the bending curve for a piezoelectric bimorph to verify the accuracy and precision (Fig 4).^{1,2} Figures 6 and 7 verify that sub-nanometer d.c.

(and slowly time varying) displacements can be measured with this method. While we have found that the combination of PSI and LFI has produced a robust measuring technique, we have also observed several nuances of its behavior. We have observed systematic oscillations in the determination of the fringe visibility and the optical path length caused by the breakdown of the assumption that multiple reflections can be ignored; we have developed a model to describe this error.^{1,2}

Our preliminary measurement of the static contact angle of PDMS on fluorinated silicon agree with the literature, however, we have not yet determined the precision of this measurement. Since the phase changes rapidly at the edge of the drop, high spatial resolution is required to adequately sample the phase. As further calibration of the technique, we intend to measure a range of contact angles.

ACKNOWLEDGEMENTS

This work is funded under a MSAD Advanced Technology Development Grant to NASA Lewis. We thank Jeff Mackey (NYMA, Inc.) for providing the index of refraction of PDMS.

REFERENCES

1. Ovrn, B; Andrews, J.H., Eppell, S. and Khaydarov, J.: Phase-shifted, real-time laser feedback interferometry, SPIE Vol. 2860, 1996, pp 263-275.
2. Ovrn, B; Andrews, J.H., and Eppell, S: Phase-measuring laser feedback interferometry: applications to microscopy, SPIE Vol. 2655, 1996, pp 153-163.
3. Extrand, C.W: Spontaneous spreading of viscous liquid drops, J. Colloid and Interface Sci, 157, 1993, 72-76.
4. Schulz, G. and Ellsner, K. E.: Errors in phase-measurement interferometry with high numerical apertures, Appl. Opt. 30, 1991, 4500- 4506.

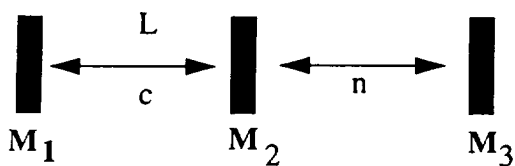


Figure 1. Model for the effect of feedback from the sample, represented by M_3 .

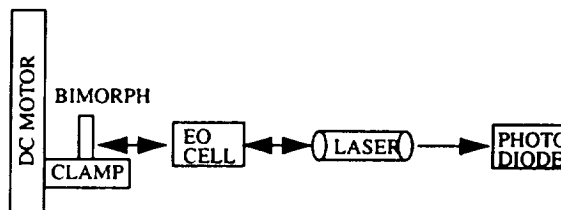


Figure 2. Schematic diagram of the LFI used to measure cantilever bending of the bimorph.

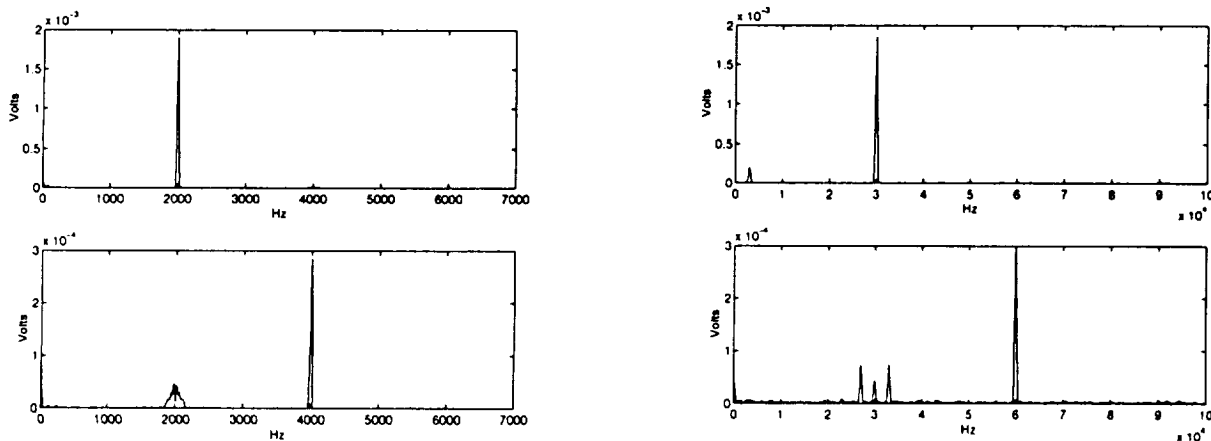


Figure 3. The harmonic response of the interferometer when the EOM was modulated at 2 kHz with the sample (mirror) held stationary (left) and with the EOM oscillating at 30 kHz and the mirror at 2 kHz (right). Changing the dc offset to the EOM was used to maximize either the fundamental (top) or second harmonic (bottom).

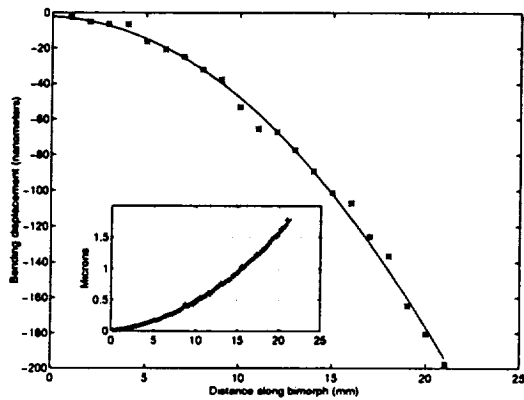


Figure 4. Bending curves for the bimorph for when two separate voltages were applied: 4.0 V (inset) and -500 mV.

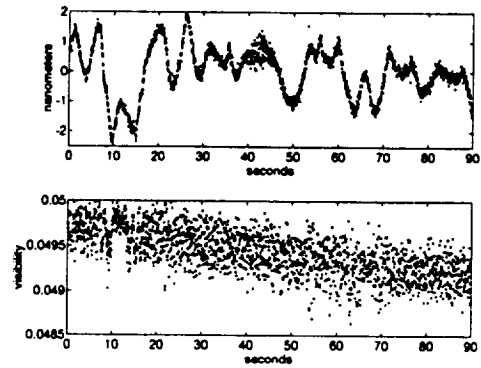


Figure 5. Drift in the optical path and visibility during a 90 second period. The visibility was essentially constant during this period.

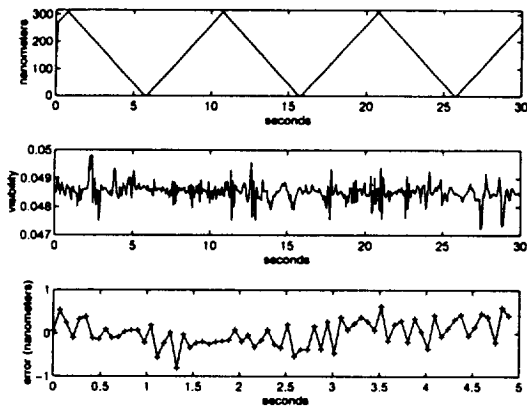


Figure 6. OPL variation caused by a 0.1 Hz ramp applied to the EOM (top). Also shown is the fringe visibility (middle) and the phase error (bottom). The phase error was calculated from the difference between a data and a least squares line.

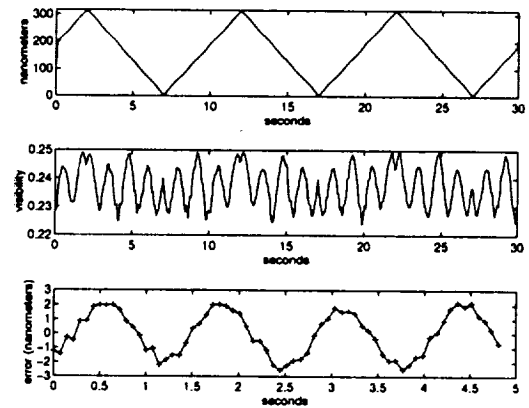


Figure 7. OPL variation caused by a 0.1 Hz ramp applied to the EOM (top) when the visibility was set to the maximum value. Also shown is the fringe visibility (middle) and the phase error (bottom).

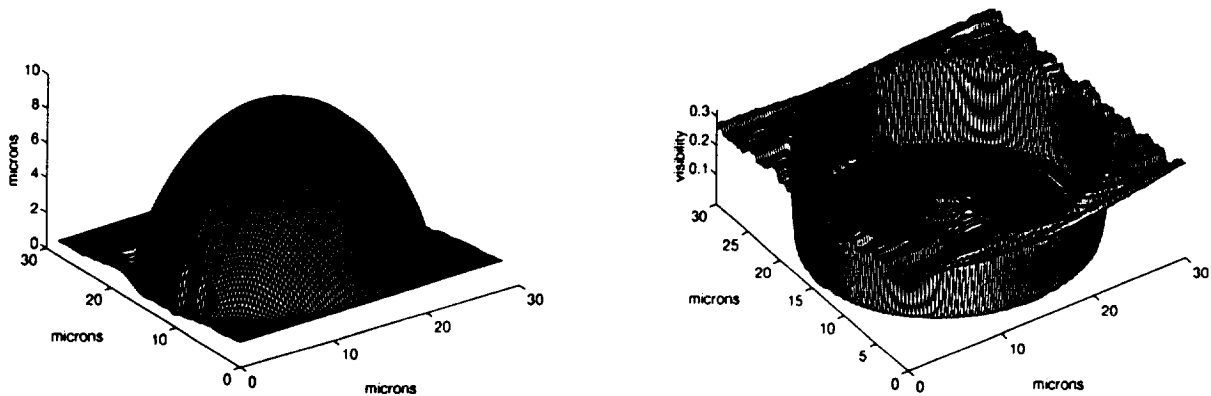


Figure 8. OPL (left) and visibility (right) variation across a static PDMS drop on fluorinated silicon wafer. The image was produced using a 50 x 0.8 NA objective. Scanning time was about 50 msec/data pixel; the images are 240 x 240 pixels.